Fabrication and Magnetic Properties of Ni Nanospheres Encapsulated in a Fullerene-like Carbon

S. V. Pol,[†] V. G. Pol,[†] A. Frydman,[‡] G. N. Churilov,[§] and A. Gedanken*,[†]

Department of Chemistry and Kanbar Laboratory for Nanomaterials at the Bar-Ilan University Center for Advanced Materials and Nanotechnology, and Department of Physics, Bar-Ilan University, Ramat-Gan, 52900, Israel, and L.V. Kirensky Institute of Physics SB RAS, Akademgorodok, Krasnoyarsk, 660036, Russia

A very simple, efficient, and economical synthetic technique, which produces fascinating fullerene-like Ni−C (graphitic) core−shell nanostructures at a relatively low temperature, is reported. The thermal dissociation of Ni acetylacetonate is carried out in a closed vessel cell (Swagelok) that was heated at 700 °C for 3 h. The encapsulation of ferromagnetic Ni nanospheres into the onion structured graphitic layers is obtained in a one-stage, single precursor reaction, without a catalyst, that possesses interesting magnetic properties. The magnetoresistance (MR) property of Ni nanospheres encapsulated in a fullerene-like carbon was measured, which shows large negative MR, of the order of 10%. The proposed mechanism for the formation of the Ni−C core−shell system is based on the segregation and the surface flux formed in the Ni and carbon particles during the reaction under autogenic pressure at elevated temperature.

Introduction

Magnetic nanomaterials have been intensively studied in recent years with respect to their novel properties and commercially potential valuable applications. The application of the encapsulated magnetic nanomaterials ranges from magnetic inks, magnetic recording media, a toner for xerography, to ferrofluids for biomedical applications, such as contrast agents in magnetic resonance imaging.[1] The ferromagnetic nanosized Fe, Ni, or Co coated with carbon constitute the group of especially interesting magnetic nanomaterials. This is because of their fascinating magnetic properties and the carbon coating, which protects the magnetic nanoparticles against environmental degradation.[2] Graphitic nanotubes[3] were first observed by Iijima during the direct-current arc discharge between graphite electrodes in an argon environment. Typical temperatures for graphitic carbon nanotube production by that method are in the range of 2000−3500 °C. Since their discovery, various authors have described alternative means for lowering the temperature[4] for the synthesis of carbon nanotubes and encapsulated nanoparticles.[5]

A novel, chemical vapor deposition method has been developed to synthesize super-long continuous Ni nanowires encapsulated in carbon nanotubes by using cloth-like SWNT raw soot as a catalyst.[6] The growth of carbon nanotubes, achieved by chemical vapor deposition, and the effect of different gases used for the catalyst surface pretreatment (N₂, H₂, or NH₃) were also analyzed. It proved that the nanotube nucleation and growth[7] processes depend strongly on the film thickness of the Ni catalyst and on the conditions of the surface treatment/cleaning before growth. In another study, carbon nanostructures have been selectively grown directly on the top of a nickel ion implanted nanopyramid array by plasma-enhanced chemical vapor deposition[8] through the anisotropic etching of silicon in hydrazine. Ping-Zhan et al. synthesized carbon-coated iron and nickel nanocapsules[9] produced by arc discharge in ethanol vapor. The copper and nickel acetylacetonates were used as the catalysts and carbon monoxide as precursor for the synthesis of carbon nanotubes and onion particles.[10] The carbon nanotubes and onions were formed in the presence of nickel particles in the temperature range of 923−1216 °C.

In the current article, we report a simple, efficient, and economical synthesis technique for the fabrication of fullerene-like Ni−C core−shell (NCCS) nanostructures. The onion-like, core−shell nanostructure is obtained in a one-stage, solvent free, single precursor reaction, without a catalyst. In addition, the reaction is conducted at a relatively low temperature, 700 °C, as compared to other methods for the formation of graphitic layers. The graphitic layers surround a ferromagnetic Ni core that possesses the large negative MR, of the order of 10%. We have named such reactions RAPET (reactions under autogenic pressure at elevated temperature) and have already reported on a variety of RAPET reactions of organic and inorganic precursors. The materials produced by this method include mono-dispersed, 2.5 ± 0.05 μm carbon spherules,[11] Si coated on spherical carbon,[12] metastable phases of Co and ZrO₂ nanoparticles,[13] the encapsulation of a superconducting material, MgCNi₃, in a carbon nanoflask,[14] as well as core−shell structures of metals/metal oxides with carbon.[15] The effects of an applied magnetic field on the RAPET of MoO(OMe)₄[16] and mesitylene[17] are also reported.

Experimental Section

1. Synthesis of Onion-like Ni−C Core−Shell Nanostructures. The synthesis of Ni−C (graphitic) core−shell nanostruc-

* Corresponding author. Fax: +972-3-5351250. E-mail: gedanken@mail.biu.ac.il.

† Department of Chemistry and Kanbar Laboratory for Nanomaterials at the Bar-Ilan University Center for Advanced Materials and Nanotechnology, Bar-Ilan University.

‡ Department of Physics, Bar-Ilan University.

§ L.V. Kirensky Institute of Physics SB RAS.

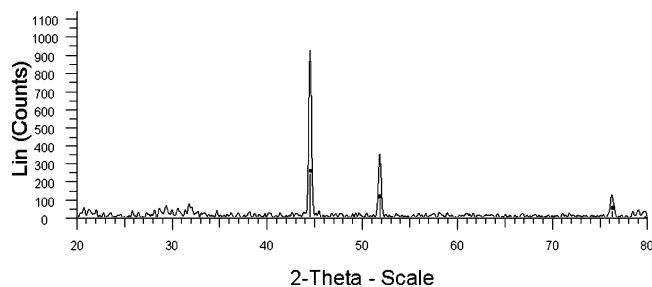**Figure 1.** XRD pattern of Ni−C core−shell nanostructures.

Figure 2. The transmission electron micrographs of (a) Ni−C core−shell nanostructures; (b) HR-TEM image of Ni−C core−shell, SAEDX carried out on the marked area; (c) Ni core is covered with ∼15−20 nm size carbon shell and the interlayer spacing of graphitic carbon; (d) interlayer spacing of Ni core (inset: electron diffraction obtained from the Ni core); and (e) SEM image of NCCS sample.

tures is carried out by the thermal dissociation of nickel acetylacetonate, $Ni(C_5H_7O_2)_2$, which was purchased from the Across Chem. Co. and used as received. The 3 mL closed vessel cell was assembled from stainless steel Swagelok parts. A $^1/_2$” union part was plugged from both sides by standard caps. For this synthesis, 1 g of nickel acetylacetonate was introduced into the cell at room temperature under nitrogen (glovebox). The filled cell was closed tightly by the other plug and then placed inside an iron pipe at the center of the tube furnace. The temperature was raised at a heating rate of 10 °C per minute. The closed vessel cell was heated at 700 °C for 3 h. The reaction took place at an autogenic pressure of the precursor. The closed vessel cell (Swagelok) was gradually cooled (∼5 h) to room temperature, opened with the release of a little pressure, and 0.513 g of a black powder was obtained. The product is termed as NCCS (Ni−C core−shell) nanostructures. The products are directly characterized by various structural, compositional, morphological, and magnetic techniques without further processing.

2. Characterizations. XRD patterns were collected by using a Bruker AXS D* Advance Powder X-ray diffractometer (Cu Kα radiation, wavelength 1.5406 Å). The morphologies and nanostructure were further characterized with a JEM-1200EX TEM model and a JEOL-2010 HR-TEM model using an accelerating voltage of 80 and 200 kV, respectively. SAEDS (selected area energy dispersive X-ray analysis) of one individual particle was conducted using a JEOL-2010 HR-TEM model, and SAEDX was done by using an X-ray microanalyzer (Oxford Scientific). The elemental analysis of the samples was carried out by an Eager 200 C, H, N, S analyzer. The Olympus BX41 (Jobin Yvon Horiba) Raman spectrometer was employed, using the 514.5 nm line of an Ar laser as the excitation source to analyze the nature of the carbon present around the Ni particle. A Micromeritics (Gemini 2375) surface area analyzer was used to measure the surface area of NCCS sample. The encapsulated Ni nanospheres maintain ferromagnetic properties, confirmed by magnetization and magnetoresistance (MR) measurements. DC magnetization measurements were performed in a Quantum Design superconducting interference device magnetometer (MPMS). A room-temperature M−H curve is also presented. The NCCS sample powder was pressed using 4-ton pressure to form a pellet.

Results and Discussion

1. X-ray Diffraction and C,H,N, S Analysis. An X-ray diffractogram for the NCCS sample is shown in Figure 1. The major peaks appear at 2θ values of 44.5°, 51.77°, and 76.2°, which correspond to the reflection lines of the face-centered cubic phase of Ni. These values are in agreement with the diffraction peaks, peak intensities, and cell parameters of crystalline fcc Ni (PDF No. 03-065-2865). Only the FCC peaks from the Ni core are observed, however; the HCP peaks are not observed.
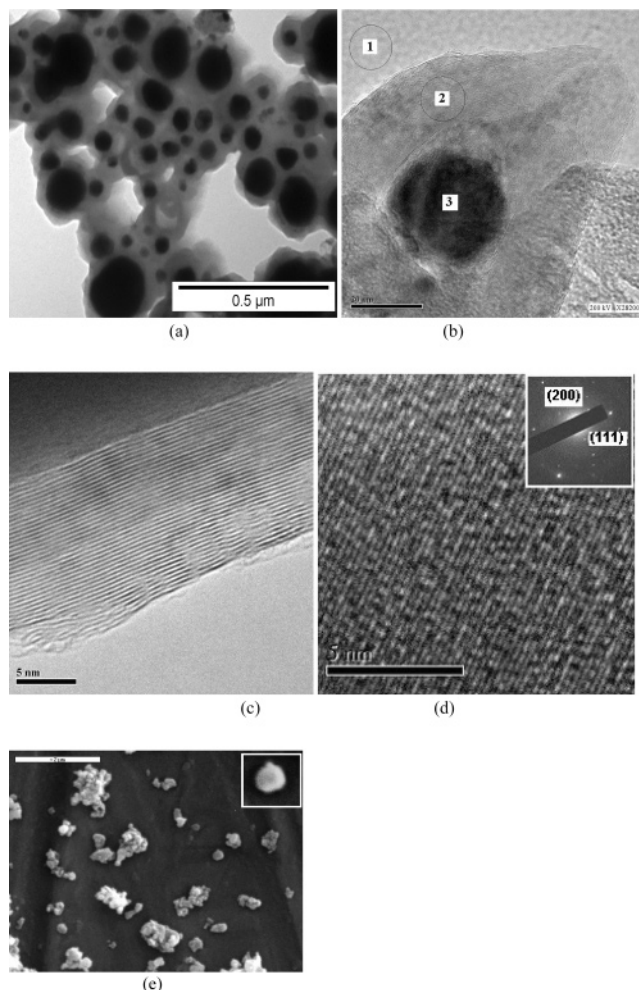
The calculated elemental (wt) percentages of Ni, C, H, and O in the $Ni(C_5H_7O_2)_2$ precursor are 22.86%, 46.74%, 5.5%, and 24.9%, respectively. We could determine the carbon and hydrogen content in the NCCS product by elemental [C,H,N,S] analysis. The measured amount of carbon in the NCCS sample is 42%, while the amount of hydrogen is reduced to 1.0%. Here, the presence of carbon and hydrogen in the NCCS sample is reduced, because during the decomposition of the precursor, gases such as C_xH_y (hydrocarbons) and/or H_2 are formed. These gases are liberated upon the opening of the closed vessel cell (Swagelok).

2. TEM, HR-TEM, SAEDS, Raman Spectroscopy, and BET Surface Area Measurements. The morphology of the NCCS sample was studied by TEM measurements. It shows spherical particles coated with nanolayers of a contrasting material. The diameters of these cores range between 30 and 180 nm (Figure 2a). The core sizes varied, but most of the particles are covered with a uniform carbon shell, which helps to stabilize the Ni core and does not allow a change in the oxidation state of Ni at room temperature. The three-dimensional onion-like structure was demonstrated when the TEM grid was tilted and the picture remained unchanged.

The assignments of the Ni core and the carbon shell nanostructure are based on SAEDS analysis. We focused a 25
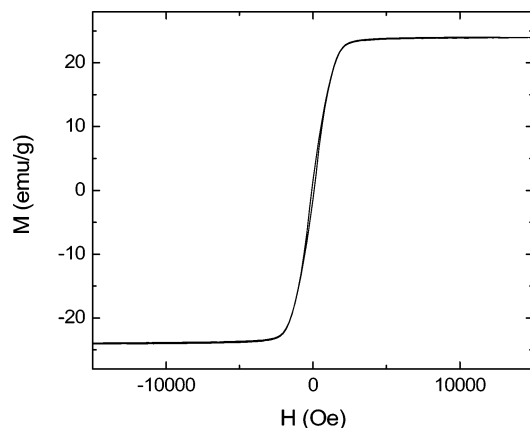
Figure 3. Magnetization versus magnetic field curve for a NCCS sample.

Figure 4. Magnetoresistance defined as $[R(\mathrm{H}) - R(0)]/R(0)*100$ of a NCCS sample. The thick line represents a field sweep from left to right, and the thin line represents a sweep from right to left. The sample resistance was 120 Ω.

nm electron beam on the various marked parts of the NCCS particle to understand its composition (Figure 2b). The SAEDS of the contrasting material (edge, marked by digit 2) shows the presence of C and Cu, and is identified as carbon, which covers the central part. The intensity of the carbon presence, depicted from the part marked by digit 2, is higher than the bare, carbon-coated Cu grid, marked by digit 1. However, the typical SAEDS of the dark (center, marked by digit 3) part of the NCCS particle shows the presence of Ni, C, and Cu and is identified as the Ni core. The presence of Cu is from the Cu grid that is used for the TEM sample preparation. The picture at higher magnification shows that the Ni core (Figure 2c) is decorated with uniform graphitic carbon shells. The image taken at the edge of the NCCS sample shows an ordered graphitic carbon shell of ~15 nm. The interlayer spacing between these graphitic planes is 3.41 Å, which is very close to that of the graphitic layers. The HR-TEM is depicted in Figure 2d and provides further verification for the identification of the core as Ni. It illustrates the perfect arrangement of the atomic layers and the lack of defects. The measured distance between these (111) lattice planes is 0.200 nm, which is very close to the distance between the planes reported in the literature (0.203 nm) for the face-centered cubic lattice of the Ni (PDF No. 03-065-2865). A selected area electron diffraction for the Ni particle is presented (inset), and the identified planes are highlighted. A typical SEM image is shown in Figure 2e, indicating the spherical morphology of the NCCS particles. The NCCS particles have a tendency to form a few agglomerates, which are observed in addition to individual particles. The aggregation is attributed to their magnetic nature. The separated particles are of ~200 nm diameter. The high-resolution image (shown in inset) depicts the spherical shape of a single NCCS particle.

Because the NCCS product contains about a 42 element % of carbon, Raman spectroscopy measurements were performed to understand the nature of the coated carbon. The two characteristic bands of carbon were detected at 1344.11 cm^{-1} (D- band) and at 1590.97 cm^{-1} (G-band)[18] for the NCCS product. The intensity of the G-band associated with graphitic carbon is more intense than the D-band associated with disordered carbon. This presence of disordered carbon might arise from the bare carbon present in the NCCS product. The Brunauer−Emmett−Teller (BET) surface area of the NCCS sample, which is prepared at 700 °C, is 75.6 m²/g.

3. Magnetic Properties. The NCCS particles exhibit typical ferromagnetic curves with a saturation magnetization of 23.5 emu/g (Figure 3). Taking into account that the sample contains 58% of Ni, this gives a value of 40 emu/g, which is close to
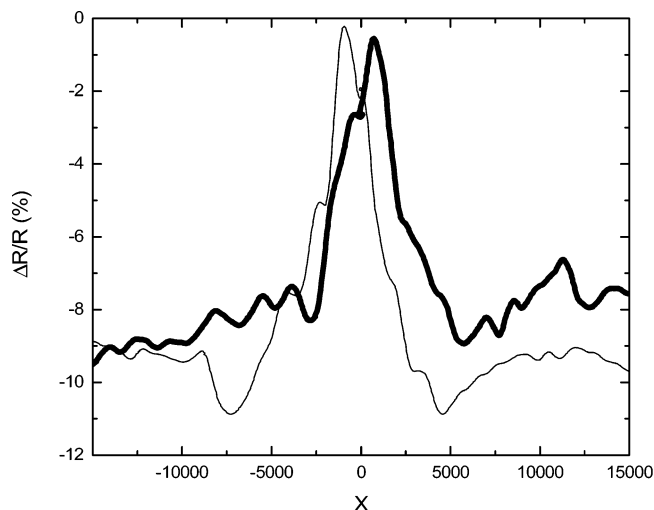
the bulk value of Ni (~50 emu/g). That the value is slightly smaller than the bulk value is not surprising. Nanomagnetic particles are expected to exhibit reduced magnetization due to the large percentage of surface spins, with disordered magnetization orientation.[19] It is expected to have very large saturation magnetization, thus giving rise to suppressed magnetization. The fact that the magnetization is smaller than that resulting from the bare Ni particles indicates that there is no magnetic proximity effect between ferromagnetic Ni and carbon, which is consistent with recent experiments.[20] Such a proximity effect was proposed as a possible explanation for ferromagnetism in carbon.[21,22]

Magnetoresistance measurements were carried out on the pellet of a NCCS sample. Figure 4 depicts resistance versus magnetic field of such a pellet at $T = 4$ K.

The MR curves show large negative MR, of the order of 10%. Although, to our knowledge, the MR properties of Ni nanospheres in a C matrix were not measured before, our results are typical for a high-quality system of ferromagnetic nanoparticles embedded in a metallic matrix.[23−25] Such behavior was ascribed to the alignment of the particle moments in the direction of *H*. A saturation field of 0.5 T, and a 4 K coercive field of the order of 100 Oe, are characteristic values for Ni particles with diameters of 10−20 nm.[26]

Mechanistic Elucidation

From TEM, HR-TEM, SAEDS, and Raman spectroscopy analysis, it is clear that the NCCS product, after the thermal dissociation of Ni(C$_5$H$_7$O$_2$)$_2$, is composed of a Ni core surrounded by graphitic carbon. The thermal decomposition of Ni-(C$_5$H$_7$O$_2$)$_2$ takes place at a temperature above 300 °C, forming a vapor[10] of Ni and carbon. The next stage is the formation of metallic nickel particles by vapor nucleation and condensation, and particle coagulation processes. At the high-temperature zone, the process of the dissolution of the released carbon in the nickel particles[10] occurs. Note that at some point the particles become saturated by carbon due to either the carbon solubility limit or the temperature decrease. The final product of the reaction is determined during the cooling and is related to carbon segregation in the supersaturated particles due to the reduction in solubility as the system's temperature decreases. The dissolved carbon contributes to the flux of carbon atoms to the particle surface upon cooling. This is called the segregation flux.

Additionally, there is another flux, the surface flux, which is limited by the diffusion of carbon atoms on the surface of the particles seeking their lowest energy states. If the cooling rate is infinitely slow, then the achieved particle structure after carbon segregation would be graphitic carbon around a nickel particle, that is, the equilibrium structure.[10] However, due to competition between the segregation and surface fluxes, two situations can occur in the system upon cooling. When the segregation flux is smaller than the surface flux, the initiation of CNT growth can occur, because there is insufficient time for the creation of the equilibrium structure. In this case, nucleation of the CNTs is likely to occur from islands where the segregation flux is larger. Gavillet et al. have shown the existence of such conditions.[27] When the segregation flux is smaller than the surface flux, carbon forms the thermodynamically most stable system, that is, particles surrounded by graphitic layers. This situation can be realized experimentally at residence times of less than 3.0 s and in the presence of nitrogen, where particles appear with graphitic shells.[10] The present thermal dissociation of Ni (acac)$_2$ at 700 °C produces graphitic carbon shell around the Ni core. This temperature is comparatively lower than the reported temperatures in other experiments,[9,10] because the present reaction is carried out under the autogenic pressure of the precursor at elevated temperature.

Conclusions

The Ni−C core−shell nanostructure is fabricated in a one-stage, solvent free, single precursor reaction, without a catalyst, at 700 °C. Our mechanistic elucidation for a Ni−C core−shell system is based on the segregation and the surface flux formed between the Ni and carbon particles during the reaction under autogenic pressure at elevated temperature. The MR property of Ni nanospheres in a C matrix was measured, which shows large negative MR, of the order of 10%.

References and Notes

(1) Kim, D. K.; Zhang, Y.; Kehr, J.; Lason, T. K.; Bjelke, B.; Muhammed, M. *J. Magn. Mater.* **2001**, *225*, 30.

(2) Leonhardt, A.; Ritschel, A. M.; Kozhuharova, R.; Graff, A.; Muhl, T.; Huhle, R.; Monch, I.; Elefant, D.; Schneider, C. M. *Diamond Relat. Mater.* **2003**, *12*, 790.

(3) Iijima, S. *Nature* **1991**, *354*, 56.

(4) Hafner, J. H.; Bronikowski, M. J.; Azamian, B. R.; Nikolaev, P.; Rinzler, A. G.; Colbert, D. T.; Smith, K. A.; Smalley, R. E. *Chem. Phys. Lett.* **1998**, *296*, 195.

(5) Jiao, J.; Seraphin, S. *J. Phys. Chem. Solids* **2000**, *61*, 1055.

(6) Guan, L.; Shi, Z.; Li, H.; You, L.; Gu, Z. *Chem. Commun.* **2004**, 1988.

(7) Moshkalyov, S. A.; Moreau, A. L. D.; Guttitérrez, H. R.; Cotta, M. A.; Swart, J. W. *Mater. Sci. Eng., B* **2004**, *112*, 147.

(8) Ferrer, D.; Shinada, T.; Tanii, T.; Kurosawa, J.; Zhong, G.; Kubo, Y.; Okamoto, S.; Kawarada, H.; Ohdomari, I. *Appl. Surf. Sci.* **2004**, *234*, 72.

(9) Si, P.-Z.; Zhang, Z.-D.; Geng, D.-Y.; You, C.-Y.; Zhao, X.-G.; Zhang, W.-S. *Carbon* **2003**, *41*, 247.

(10) Nasibulin, A. G.; Moisala, A.; Brown, D. P.; Kauppinen, E. I. *Carbon* **2003**, *41*, 2711.

(11) Pol, V. G.; Motiei, M.; Calderon-Moreno, J.; Yoshimura, M.; Gedanken, A. *Carbon* **2004**, *42*, 111.

(12) Pol, V. G.; Pol, S. V.; Gedanken, A.; Goffer, Y. *J. Mater. Chem.* **2004**, *14*, 966.

(13) Pol, S. V.; Pol, V. G.; Seisenbaeva, G.; Kessler, V. G.; Gedanken, A. *Chem. Mater.* **2004**, *16*, 1793.

(14) Rana, R. K.; Pol, V. G.; Felner, I.; Meridor, E.; Frydman, A.; Gedanken, A. *Adv. Mater.* **2004**, *16*, 972.

(15) Pol, S. V.; Pol, V. G.; Gedanken, A. *Chem.-Eur. J.* **2004**, *10*, 4467.

(16) Pol, S. V.; Pol, V. G.; Kessler, V. G.; Seisenbaeva, G. A.; Sung, M.-G.; Asai, S.; Gedanken, A. *J. Phys. Chem. B* **2004**, *108*, 6322.

(17) Pol, V. G.; Pol, S. V.; Gedanken, A.; Sung, M.-G.; Shigeo, A. *Carbon* **2004**, *42*, 2738.

(18) Jeong, S.-H.; Ko, J.; Park, J.-B; Par, W. *J. Am. Chem. Soc.* **2004**, *126*, 15982.

(19) Kodoma, H. R.; Berkovitz, A. E.; Mcniff, E. J., Jr.; Foner, S. *Phys. Rev. Lett.* **1996**, *77*, 394.

(20) Höhne, R.; Ziese, M.; Esquinazi, P. *Carbon* **2004**, *42*, 3109.

(21) Coey, J. M. D.; Venkatesan, M.; Fitzgerald, C. B.; Douvalis, A. P.; Sanders, I. S. *Nature* **2002**, *420*, 156.

(22) Cespedes, O.; Ferreira, M. S.; Sanvito, S.; Cosiak, M.; Coey, J. M. D. *J. Phys.: Condens. Matter* **2004**, *16*, L155.

(23) Berkowitz, A. E.; et al. *Phys. Rev. Lett.* **1992**, *68*, 3745.

(24) Xiao, J. Q.; Jiang, J. S.; Chien, C. L. *Phys. Rev. Lett.* **1992**, *68*, 3749.

(25) Wang, J. Q.; Xiong, P.; Xiao, G. *Phys. Rev.* **1993**, *B47*, 8341.

(26) Frydman, A.; Dynes, R. C. *Solid State Commun.* **1999**, *110*, 485.

(27) Gavillet, J.; Loiseau, A.; Ducastelle, F.; Thair, S.; Bernier, P.; Stephan, O. *Carbon* **2002**, *40*, 1649.